

Catalytic H/D Exchange between Organic Compounds and D₂O with TpRu(PPh₃)(CH₃CN)H (Tp = hydro(trispyrazolyl)borate). Reaction of TpRu(PPh₃)(CH₃CN)H with Water to Form Acetamido Complex TpRu(PPh₃)(H₂O)(NHC(O)CH₃)

Chung Wing Leung,[†] Wenxu Zheng,[‡] Dexian Wang,[†] Siu Man Ng,[†] Chi Hung Yeung,[†] Zhongyuan Zhou,[†] Zhenyang Lin,^{*,‡} and Chak Po Lau^{*,†}

Department of Applied Biology and Chemical Technology, The Hong Kong Polytechnic University, Hung Hom, Kowloon, Hong Kong, People's Republic of China, and Department of Chemistry, The Hong Kong University of Science and Technology, Clear Water Bay, Kowloon, Hong Kong, People's Republic of China

Received November 14, 2006

Deuteration of organic molecules using D₂O as the deuterium source is affected with catalytic systems based on the ruthenium solvento hydride complex TpRu(PPh₃)(CH₃CN)H. The deuteration reactions can be performed under Ar or H₂. In the former case, the hydride ligand is rapidly deuterated by D₂O, and in the course of the catalysis, D₂O converts TpRu(PPh₃)(CH₃CN)D into the acetamido complex TpRu(PPh₃)(D₂O)(NDC(O)CH₃), which at the later stage of the reaction generates two additional minor species, one of which is the partially deuterated carbonyl hydride species TpRu(PPh₃)(CO)H(or D). All of these complexes are, however, found to be inactive for the H/D exchange reactions between the organic molecules and D₂O. In the exchange reactions under H₂, a mixture of the HD isotomers, TpRu(PPh₃)H_{3-x}D_x, of the dihydrogen hydride complex TpRu(PPh₃)(H₂)H are the active species. On the basis of our previous work on the TpRu(PPh₃)(CH₃CN)H-catalyzed H/D exchange reactions between deuterated organic molecules and CH₄, it is proposed that TpRu(PPh₃)(CH₃CN)D and TpRu(PPh₃)(H_{3-x})D_x exchange their deuteride ligands Ru–D with R–H via the intermediacies of the η²-R–H(or D) and η²-H–H(or D) σ-complexes; the Ru–H bonds thus formed after the exchange are deuterated by D₂O to regenerate the metal deuterides. The solvento complex TpRu(PPh₃)(CH₃CN)D under Ar is suggested to be more active than TpRu(PPh₃)(H_{3-x})D_x under H₂ for the H/D exchange reactions because the former reacts more readily with the organic molecule R–H to generate the η²-R–H σ-complex due to higher lability of the CH₃CN ligand in comparison with the dihydrogen or hydrogen–deuterium ligand of TpRu(PPh₃)(H_{3-x})D_x. The acetamido complex TpRu(PPh₃)(H₂O)(NHC(O)CH₃) was independently prepared by refluxing a THF solution of TpRu(PPh₃)(CH₃CN)H containing excess water for 24 h, and its molecular structure was determined by X-ray crystallography. Theoretical calculations at the Becke3LYP level of DFT theory have been performed to study the reaction of TpRu(PPh₃)(CH₃CN)H with H₂O that leads to the formation TpRu(PPh₃)(H₂O)(NHC(O)CH₃). It is shown that the hydration reaction is promoted by a Ru–H···H–OH dihydrogen-bonding interaction between the hydride ligand and the attacking water molecule. An explanation for the failure of the chloro analogue TpRu(PPh₃)(CH₃CN)Cl to react with water to form the acetamido complex is also provided.

Introduction

Incorporation of deuterium into C–H bonds of organic molecules is important to preparative chemistry of deuterium-labeled materials, which have a number of important uses from solvents for NMR spectroscopy to reagents for mechanistic investigation. Deuterium oxide, due to its low cost and low toxicity, is an attractive isotopic source. However, metal-catalyzed H/D exchange between C–H bonds and D₂O is relatively rare.¹ Tilley, Bergman, and co-workers have recently reported that the iridium complex Cp*(PMe₃)IrCl₂ shows promising results in catalyzing the exchange of deuterium from

D₂O into organic molecules without added acids or stabilizers.² The O-donor iridium–methoxyl complexes [Ir(acac-O,O)₂(OMe)(L)] (L = pyridine or CH₃OH) have been found to catalyze H/D exchange between D₂O and C₆H₆ at 160 °C, albeit with very low turnover frequencies. It is anticipated that the Ir–OCH₃ is converted to the hydroxyl species Ir–OH, which reversibly activates the C–H bonds of benzene, generating Ir–Ph and water.³ It has also been reported that rhodium complexes containing aryl–PCP type ligands are able to promote catalytic

* Corresponding authors. (Z.L.) Fax: (+852) 2358-1594. E-mail: chzlin@ust.hk. (C.P.L.) Fax: (+852) 2364-9932. E-mail: bccplau@polyu.edu.hk.

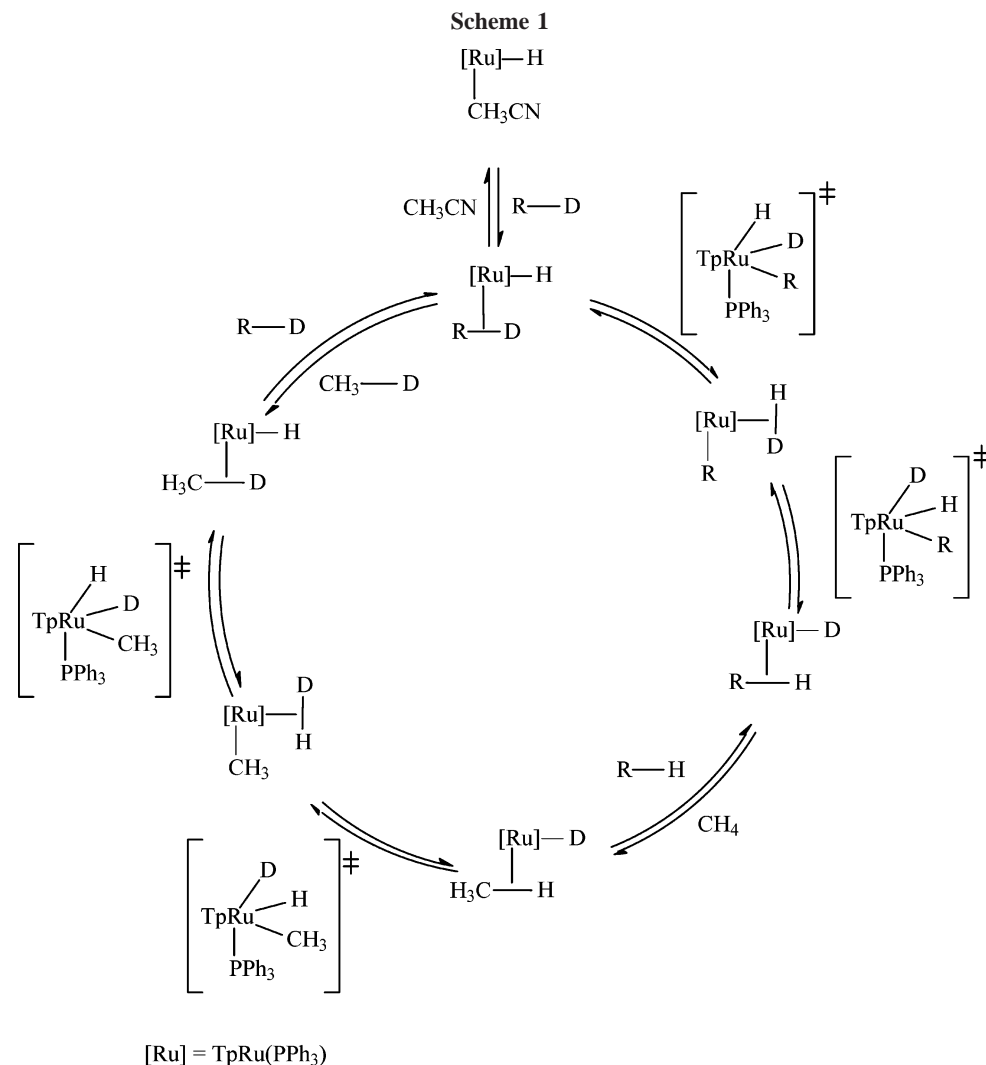
[†] The Hong Kong Polytechnic University.

[‡] The Hong Kong University of Science and Technology.

(1) (a) Garnett, J. L.; Hodges, R. J. *J. Am. Chem. Soc.* **1967**, *89*, 4546. (b) Garnett, J. L.; Long, M. A.; McLaren, A. B.; Peterson, K. B. *J. Chem. Soc., Chem. Commun.* **1973**, 749. (c) Garnett, J. L.; West, J. C. *Aust. J. Chem.* **1974**, *27*, 129. (d) Shilov, A. E.; Shteinman, A. A. *Coord. Chem. Rev.* **1977**, *24*, 97.

(2) Klei, S. R.; Golden, J. T.; Tilley, T. D.; Bergman, R. G. *J. Am. Chem. Soc.* **2002**, *124*, 2092.

(3) Tenn, W. J., III; Young, K. J. H.; Bhalla, G.; Oxgaard, J.; Goddard, W. A., III; Periana, R. A. *J. Am. Chem. Soc.* **2005**, *127*, 14172.



H/D exchange into the vinyl C–H bonds of olefins with D_2O or CD_3OD utilized as D-donor.⁴

We have recently reported that the ruthenium complex $\text{TpRu}(\text{PPh}_3)(\text{CH}_3\text{CN})\text{H}$ (Tp = hydro(trispyrazolyl)borate) (**1**) catalyzes H/D exchange between CH_4 and some deuterated organic molecules such as benzene- d_6 , tetrahydrofuran- d_8 , diethyl ether- d_{10} , and 1,4-dioxane- d_8 . Theoretical study on the reaction mechanism suggests that the six-coordinate σ -complexes $\text{TpRu}(\text{PPh}_3)(\eta^2\text{-H-R})\text{H}$ and $\text{TpRu}(\text{PPh}_3)(\eta^2\text{-H-CH}_3)\text{H}$ are important intermediates in the exchange processes, during which reversible transformations between these σ -complexes and the dihydrogen species $\text{TpRu}(\text{PPh}_3)(\eta^2\text{-H-H})\text{R}$ and $\text{TpRu}(\text{PPh}_3)(\eta^2\text{-H-H})(\text{CH}_3)$, respectively, are the crucial steps. All these transformations, however, go through transition states corresponding to the seven-coordinate species $\text{TpRu}(\text{PPh}_3)(\text{R})(\text{H})(\text{D})$ and $\text{TpRu}(\text{PPh}_3)(\text{CH}_3)(\text{H})(\text{D})$ (Scheme 1).⁵

Continuing our research on C–H bond activation, we studied the **1**-catalyzed deuteration of C–H bonds of organic molecules, using D_2O as the deuterium source. It has been briefly mentioned in recent reports that a similar Tp -ruthenium complex $\text{TpRu}(\text{PMe}_3)_2\text{OH}$ is able to promote H/D exchange between H_2O and deuterated arenes (C_6D_6 and $\text{C}_6\text{H}_5\text{CD}_3$); the turnovers for the exchange are, however, very low.⁶

Results and Discussion

H/D Exchange between Organic Molecules and D_2O under Ar.

The H/D exchange reactions were carried out in 5 mm Wilmad pressure-valved NMR tubes under 10 atm of argon. The argon pressure was applied to increase the boiling points of the organic compounds and D_2O so that they did not boil at the reaction temperature of 110 °C. Results of the **1**-catalyzed H/D exchange between organic molecules and D_2O under Ar are shown in Table 1. Reproducibility of the H/D exchange reactions was assured by duplicating each reaction using a different batch of catalyst. Each of the results in Table 1 is the average of two runs. In comparison with the iridium complex $\text{Cp}^*(\text{PMe}_3)\text{IrCl}_2$,² for example, 0.4 mol % of **1** is able to affect in 24 h total incorporation levels of 24 and 13% in the deuteration of Et_2O and THF, respectively, with D_2O , whereas incorporation levels with the iridium system in 40 h are 36 and 61%, respectively, but with 5 mol % catalyst. Although THF and 1,4-dioxane have much better miscibility with D_2O than the other substrates, these cyclic ethers do not seem to give higher percent deuteration of their C–H bonds. In our previous work on the **1**-catalyzed H/D exchange between CH_4 and deuterated organic compounds, it was found that the exchange reaction between C_6D_6 and CH_4 exhibits a higher degree of H/D

(4) Rybtchinski, B.; Cohen, R.; Ben-David, Y.; Martin, J. M. L.; Milstein, D. *J. Am. Chem. Soc.* **2003**, *125*, 11041.

(5) Ng, S. M.; Lam, W. H.; Mak, C. C.; Tsang, C. W.; Jia, G.; Lin, Z.; Lau, C. P. *Organometallics* **2003**, *22*, 641.

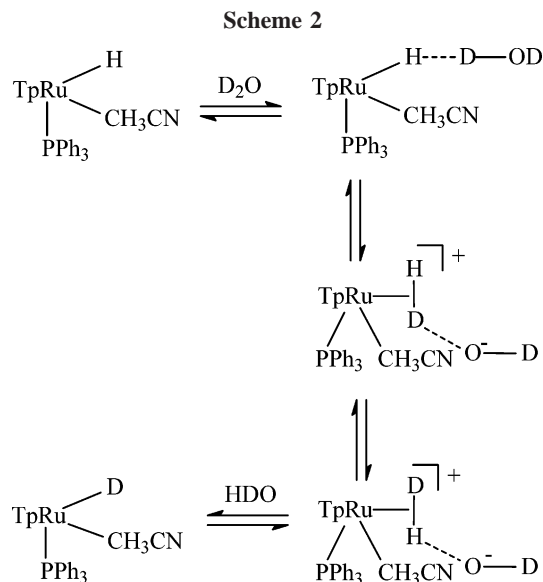
(6) (a) Feng, Y.; Lail, M.; Barakat, K. A.; Cundari, T. R.; Gunnoe, T. B.; Petersen, J. L. *J. Am. Chem. Soc.* **2005**, *127*, 14174. (b) Feng, Y.; Lail, M.; Foley, T. B.; Gunnoe, T. B.; Barakat, K. A.; Cundari, T. R.; Petersen, J. L. *Am. Chem. Soc.* **2006**, *128*, 7982.

Table 1. H/D Exchange of Organic Solvents and D₂O by **1** under Argon^a

entry	substrate	% deuteration	total TON ^b	mol % of 1 ^c	
1	benzene	27	390	0.41	
2	toluene	aliphatic:	16	256	0.48
		<i>o</i> and <i>p</i> :	16		
3	tetrahydrofuran	<i>m</i> :	12	288	0.37
		α hydrogen:	20		
4	1,4-dioxane	β hydrogen:	6	240	0.40
		α hydrogen:	12		
5	diethyl ether	α hydrogen:	19	490	0.48
		β hydrogen:	27		

^a Reaction conditions: catalyst, 0.0091 mmol; substrate, 0.2 mL; D₂O, 0.1 mL; pressure: Ar = 10 atm; temperature, 110 °C; reaction time, 24 h.

^b Total TON = mole of C–H bond activated/mole of catalyst. ^c Relative to the organic substrate



exchange than the THF-*d*₈/CH₄ and 1,4-dioxane-*d*₈/CH₄ exchange reactions. In the present study, the exchange of the α -hydrogens of THF is preferred over that of the β -hydrogens; on the other hand, the methyl hydrogens of diethyl ether undergo H/D exchange to a larger extent than the methylene hydrogens. These results are similar to the outcome of the CH₄/THF-*d*₈ and CH₄/diethyl ether-*d*₁₀ exchange reactions, which we have previously described in detail.⁵ Unfortunately, it is difficult to study the H/D exchange of aliphatic R–H with D₂O due to solubility problems of **1** in both substrates.

H/D Exchange of Ru–H with D₂O at Room Temperature.

It is noted that the hydride ligand of **1** is readily deuterated in the presence of D₂O. In a THF-*d*₈ solution, the hydride signal of **1** (δ –13.50 ppm) was easily discernible by ¹H NMR spectroscopy, and its intensity remained unaltered over an extended period of time at room temperature, indicating that the hydride ligand did not undergo H/D exchange with THF-*d*₈ at this temperature. However, the ¹H NMR spectrum of **1** taken 10 min after the addition of excess D₂O to the solution showed that the hydride signal had disappeared while all the other proton signals of the complex remained unchanged, thus indicative of fast deuteration of only the hydride ligand of **1** by D₂O at room temperature; the hydride ligand deuteration was confirmed by ²H NMR spectroscopy, which showed the Ru–D signal at δ –13.94 ppm. H/D exchange between metal hydride and D₂O has been reported.⁷ Scheme 2 shows a probable mechanism for the H/D exchange between Ru–H of **1** and D₂O. The reaction may be initiated by an interaction between the Ru–H and

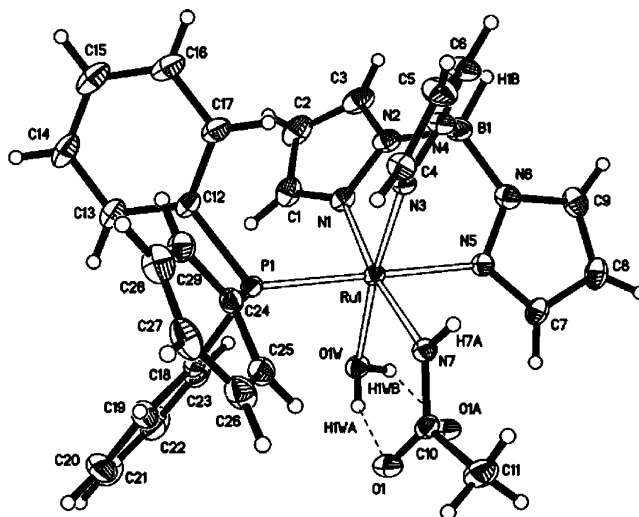


Figure 1. Molecular structure of TpRu(PPh₃)(H₂O)(NHC(O)CH₃) (**2**).

D–OD, forming a Ru–H···D–OD dihydrogen-bonded species;⁸ the H/D exchange reaction then proceeds via the intermediacies of the hydrogen-bonded ion pairs (Scheme 2). Similar mechanisms have been proposed for M–H/D₂O exchange reactions.^{7b}

Formation of TpRu(PPh₃)(D₂O)(NDC(O)CH₃) (2d**) and Structure Determination of the Ruthenium–Acetamido Complex TpRu(PPh₃)(H₂O)(NHC(O)CH₃) (**2**).** A 1-catalyzed THF/D₂O exchange reaction was monitored by ¹H and ³¹P{¹H} NMR spectroscopy. It was observed that 20 min into the catalytic reaction, approximately two-thirds of **1** was converted to the new complex **2d**, and **1** was basically not observable on the ³¹P{¹H} NMR spectrum after about 80 min. ³¹P{¹H} NMR spectroscopy showed that **2d** corresponds to a singlet at δ 62.3 ppm. ¹H NMR spectroscopy showed that the singlet corresponding to the methyl protons of the acetonitrile ligand of **1** at δ 1.93 ppm disappeared, and any new methyl signal might have been masked by the large peaks of THF. Complex **2d** remained the only detectable species by ³¹P{¹H} NMR spectroscopy for about 6 h, after which two additional species, **3** and **4**, became detectable as shown by the appearance of two minor signals at δ 68.8 and 71.5 ppm, respectively; the abundance of **3** and **4** increased at the expense of **2d**. After 15 h, **2d**, **3**, and **4** were present in approximately 2:1:1 ratio. The increase of % deuteration of the α - and β -hydrogens of THF with time was also monitored; it was observed that the percent deuteration of both types of hydrogens increased steadily with time and began to level off after about 24 h.

Complex **2** was independently prepared by refluxing a THF solution of **1** containing 150 equiv of H₂O for 24 h. Yellowish-green crystals of **2** suitable for X-ray diffraction study were obtained by slow diffusion of diethyl ether into a solution of the complex in dichloromethane. Figure 1 shows the molecular

(7) See, for example: (a) Gaus, P. L.; Kao, S. C.; Darensbourg, M. Y.; Arndt, L. W. *J. Am. Chem. Soc.* **1984**, *106*, 4752. (b) Feracin, S.; Bürgi, T.; Bakhtmutov, V. I.; Eremenko, I.; Vorontsov, E. V.; Vimenits, A. B.; Berke, H. *Organometallics* **1994**, *13*, 4194. (c) Paterniti, D. P.; Roman, P. J., Jr.; Atwood, J. D. *Organometallics* **1997**, *16*, 3371. (d) Kuo, L. Y.; Weakley, T. J. R.; Awana, K.; Hsia, C. *Organometallics* **2001**, *20*, 4969. (e) Frost, B. J.; Mebi, C. A. *Organometallics* **2004**, *23*, 5317.

(8) (a) Crabtree, R. H.; Siebbahn, P. E. M.; Eisenstein, O.; Rheingold, A. L.; Koetzle, T. F. *Acc. Chem. Res.* **1996**, *29*, 348. (b) Crabtree, R. H. *Science* **1998**, *282*, 2000. (c) Custelcean, R.; Jackson, J. E. *Chem. Rev.* **2001**, *101*, 1963. (d) Morris R. H. In *Recent Advances in Hydride Chemistry*; Peruzzini, M., Poli, R., Eds.; Elsevier: Amsterdam, 2001; Chapter 1. (e) Belkova, N. V.; Shubiua, E. S.; Epstein, L. M. *Acc. Chem. Res.* **2005**, *38*, 624.

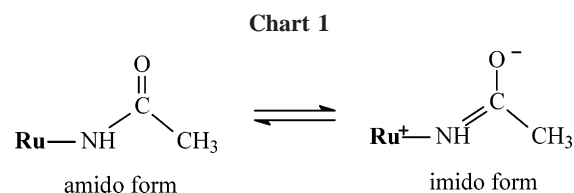
Table 2. Crystal Data and Structure Refinement for 2

empirical formula	$\text{Ru}(\text{H}_2\text{O})(\text{NHC}(\text{O})\text{CH}_3)(\text{PPh}_3)\cdot(\text{C}_9\text{H}_9\text{N}_6\text{BH})(\text{CH}_2\text{Cl}_2)$
fw	736.38
temperature	294(2) K
wavelength	0.71073 Å
cryst syst	monoclinic
space group	$P2(1)/c$
unit cell dimens	$a = 11.3769(17)$ Å $\alpha = 90^\circ$ $b = 19.318(3)$ Å $\beta = 108.474(2)^\circ$ $c = 15.830(2)$ Å $\gamma = 90^\circ$
volume	$3299.6(9)$ Å ³
Z	4
density (calcd)	1.482 Mg/m ³
absorp coeff	0.725 mm ⁻¹
$F(000)$	1500
cryst size	$0.50 \times 0.40 \times 0.40$ mm ³
θ range for data collection	$1.75\text{--}27.55^\circ$
index ranges	$-14 \leq h \leq 14$, $-25 \leq l \leq 25$, $-20 \leq k \leq 20$
no. of reflns collected	30 427
no. of indep reflns	7608 [$R(\text{int}) = 0.0342$]
completeness to $\theta = 27.55^\circ$	99.8%
absorp corr	semiempirical from equivalents
max. and min. transmn	0.9333 and 0.8923
refinement method	full-matrix least-squares on F^2
no. of data/restraints/params	7608/4/425
goodness-of-fit on F^2	1.001
final R indices [$I > 2\sigma(I)$]	$R1 = 0.0371$, $wR2 = 0.1030$
R indices (all data)	$R1 = 0.0463$, $wR2 = 0.1107$
largest diff peak and hole	0.830 and -0.476 e Å ⁻³

Table 3. Selected Bond Distances and Bond Angles for $\text{TpRu}(\text{PPh}_3)(\text{H}_2\text{O})(\text{NHC}(\text{O})\text{CH}_3)$

Bond Distances (Å)			
Ru–N(1)	2.1116(17)	Ru–N(3)	2.0419(16)
Ru–N(5)	2.1210(15)	Ru–N(7)	2.0769(17)
Ru–O(1W)	2.1393(14)	C(10)–O(1)	1.268(3)
O(1W)–O(1)	2.593(2)	C(10)–N(7)	1.303(3)
O(1W)–O(1A)	2.7411(19)	O(1W)–H(1WA)	0.9098
O(1W)–H(1WB)	0.9150		
Bond Angles (deg)			
N(3)–Ru(1)–N(1)	88.10(7)	N(3)–Ru(1)–N(5)	85.69(6)
N(3)–Ru(1)–N(7)	88.68(7)	N(3)–Ru(1)–P(1)	94.42(4)
N(1)–Ru(1)–N(5)	85.95(6)	N(1)–Ru(1)–O(1W)	93.70(6)
N(1)–Ru(1)–P(1)	93.84(4)	N(7)–Ru(1)–N(5)	85.90(6)
N(7)–Ru(1)–O(1W)	88.71(6)	N(7)–Ru(1)–P(1)	94.31(4)
N(5)–Ru(1)–O(1W)	88.53(6)	O(1W)–Ru(1)–P(1)	91.36(4)
C(10)–N(7)–Ru	130.75(14)	O(1)–C(10)–N(7)	122.86(19)
O(1)–C(10)–C(11)	117.5(2)	N(7)–C(10)–C(11)	119.6(2)

structure of **2** (the solvent molecule CH_2Cl_2 is not shown). The crystal data and refinement details are given in Table 2. Selected bond distances and angles are given in Table 3. Complex **2** contains an acetamido ligand and a coordinated water molecule; the hydrogen atoms of the aquo ligand were located and refined. The acetamido ligand can have two resonance structures, the amido form and the imido form (Chart 1). The bond distances of C(10)–O(1), 1.268(3) Å, and C(10)–N(7), 1.303(3) Å, of **2** are, respectively, longer and shorter than those of the corresponding amido-type ligands.⁹ On the other hand, these distances are shorter and longer, respectively than the corresponding C–O and C–N bond distances of the imido ligand.¹⁰ Thus, the C–O and C–N bond distances of the acetamido ligand of **2** indicate



that both the amido and imido forms have contributions to the structure. One of the hydrogen atoms of the aquo ligand is intramolecularly hydrogen-bonded to the carbonyl oxygen of the acetamido ligand, while the other hydrogen exhibits an intermolecular hydrogen-bonding interaction with the carbonyl function of the acetamido ligand of another molecule. The intra- and intermolecular O \cdots O distances are 2.593(2) Å (O(1W) \cdots O(1)) and 2.7411(19) Å (O(1W) \cdots O(1A)), respectively; these O \cdots O distances fall in the range of hydrogen-bonding interactions.¹¹

The ¹H NMR spectrum of **2** shows the N–H as a slightly broadened singlet at δ 4.67 ppm; a singlet that corresponds to the methyl proton of the acetamido ligand is seen at δ 2.05 ppm. The carbonyl carbon of the acetamido ligand appears as a singlet at δ 181.2 ppm in the ¹³C{¹H} NMR spectrum. The low carbonyl stretching frequency ($\nu_{\text{C=O}}$) = 1540 cm⁻¹ shown by IR spectroscopy corroborates the fact that the imido form makes significant contribution to the structure. A ruthenium–acetamido complex, which is effective in catalyzing the stepwise transfer hydrogenation of carbonyl compounds and imines, also exhibits a low carbonyl amide stretching frequency ($\nu_{\text{C=O}}$) = 1545 cm⁻¹.¹² The N–H stretching frequency of **2** can be observed at 3334 cm⁻¹; it is shifted to 2402 cm⁻¹ (theoretical value is 2363 cm⁻¹) for **2d**, which can be prepared by reacting **1** with D₂O instead of H₂O.

Possible Mechanisms for the Formation of 2. Formation of the acetamido ligand in **2** requires nucleophilic attack by water (or hydroxide) at the carbon center of the coordinated acetonitrile ligand of **1**. Mechanistic study of cobalt-catalyzed hydration of nitriles indicated that intramolecular metal hydroxide attack on the coordinated nitrile resulting in the formation of chelated amido is the crucial step in the catalysis.¹³ It has also been postulated that the hydration of nitriles catalyzed by the water-soluble molybdocene (MeCp)₂Mo(OH)(H₂O)⁺ occurs by an intramolecular attack of a hydroxide ligand on a coordinated nitrile.¹⁴ On the basis of the kinetic experiments, a mechanism for the palladium-catalyzed nitrile hydration reactions was proposed; in the catalysis, internal attack on the nitrile ligand by the aqua ligand and external attack on the nitrile ligand by solvent water occur at similar rates.¹⁵ Since in the present hydration reaction, there is no additional base to generate the hydroxide ion, the conversion of the acetonitrile to the acetamido ligand might involve external nucleophilic attack of the former by water. It was, however, learned that the chloro analogue of **1**, $\text{TpRu}(\text{PPh}_3)(\text{CH}_3\text{CN})\text{Cl}$, in which the nitrile carbon should be more activated toward nucleophilic attack, remained unchanged after heating a THF solution of this complex in the presence of excess water overnight. In view of this fact, we are prompted to suggest a reaction sequence shown in Scheme 3 for the hydration of **1** to form **2**. The feature of the proposed

(11) (a) Scheiner, S. *Acc. Chem. Rev.* **1994**, *27*, 402. (b) Gilli, P.; Bertolasi, V.; Ferretti, V.; Gilli, G. *J. Am. Chem. Soc.* **1994**, *116*, 909.

(12) Yi, C. S.; He, Z.; Guzei, I. A. *Organometallics* **2001**, *20*, 3641.

(13) Kim, J. H.; Britten, J.; Chin, J. *J. Am. Chem. Soc.* **1993**, *115*, 3618.

(14) Breno, K. L.; Pluth, M. D.; Tyler, D. R. *Organometallics* **2003**, *22*, 1203.

(15) Kaminskaia, N. V.; Kostić, N. M. *J. Chem. Soc., Dalton Trans.* **1996**, 3677.

(9) (a) Ilan, Y.; Kapon, M. *Inorg. Chem.* **1996**, *25*, 2350. (b) Chou, M. H.; Szalda, D. J.; Creutz, C.; Sutin, N. *Inorg. Chem.* **1994**, *33*, 1674. (c) Kobayashi, A.; Konno, H.; Sakamoto, K.; Sekine, A.; Ohashi, Y.; Iida, M.; Ishitani, O. *Chem.–Eur. J.* **2005**, *11*, 4219.

(10) Nagao, H.; Hirano, T.; Tsuboya, N.; Shiota, S.; Mukaida, M.; Ohi, T.; Yamasaki, M. *Inorg. Chem.* **2002**, *41*, 6267.

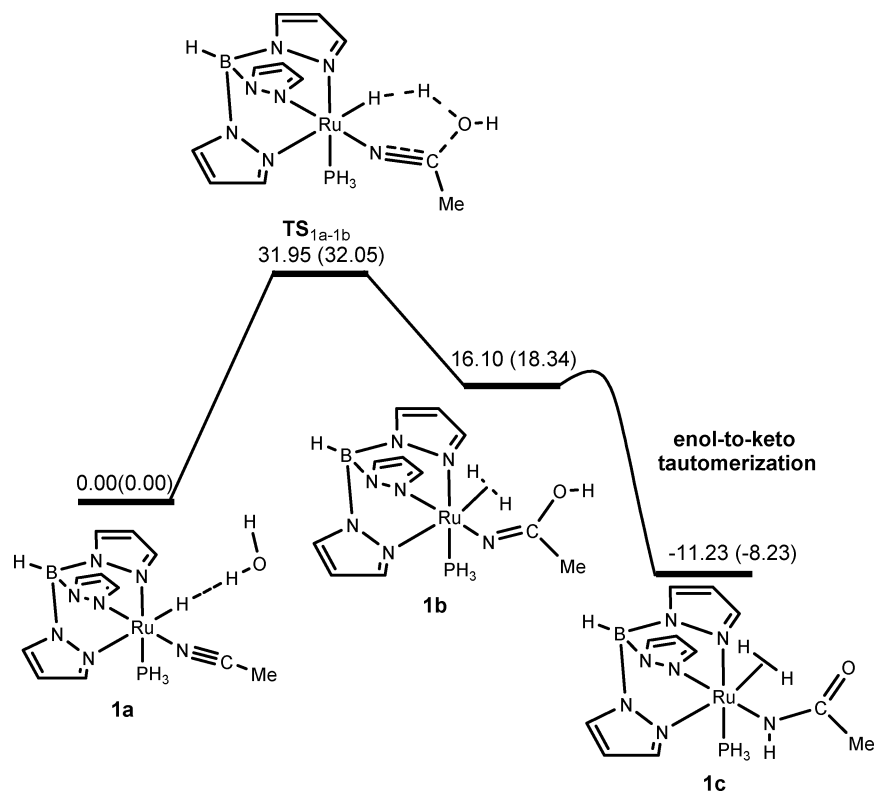
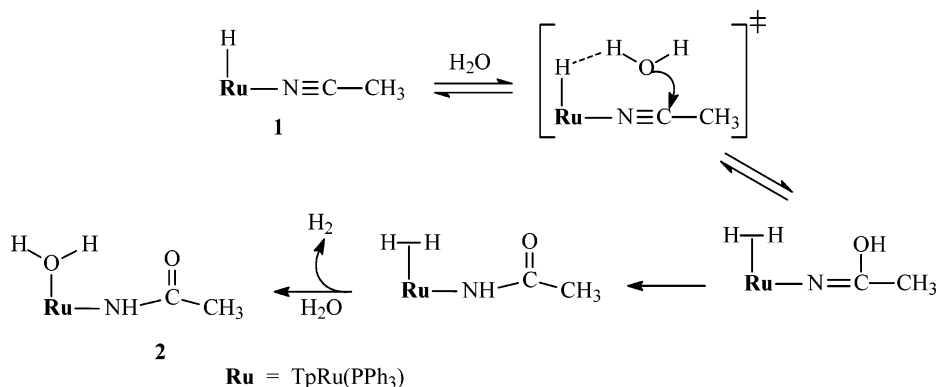


Figure 2. Energy profile for the conversion process of the acetonitrile-coordinated complex **1a** to the acetamido-coordinated complex **1c**. The calculated relative electronic energies and free energies (in parentheses) are given in kcal/mol.

Scheme 3



sequence is that the attack of water at the acetonitrile is promoted by the dihydrogen-bonding interaction of the hydride ligand of **1** with the attacking water molecule. We have recently reported a similar dihydrogen-bond-promoted catalytic hydration of nitriles with an indenylruthenium hydride complex; it was shown by density functional theory calculations that the presence of a strong $Ru-H\cdots H-OH$ interaction in the transition state lowers the barrier of the nucleophilic attack of H_2O at the carbon atom of the bound nitrile.¹⁶ Complex **1** has been found to be active in catalyzing hydration of acetonitrile to give acetamide in our preliminary study, and work on the catalytic hydration of nitriles with **1** is now in progress.

Theoretical Study. To study the feasibility of the proposed reaction mechanism shown in Scheme 3 for the reaction of hydride complex **1** with H_2O leading to the formation of complex **2**, theoretical calculations were performed at the Becke3LYP level of DFT theory to examine the most important

step corresponding to the conversion of the acetonitrile ligand to the acetamido ligand. To reduce the computer cost, PH_3 was used to model PPh_3 in our calculations.

Figure 2 illustrates the relative electronic energies ΔE and the relative Gibbs free energies ΔG° at 298 K relevant to the conversion of the acetonitrile-coordinated complex **1**, which has a dihydrogen-bonding interaction between the hydride ligand and one of the two protons of H_2O , to the acetamido-coordinated complex **1c**, having a $Ru-(\eta^2-H_2)$ bond. As shown in Figure 2, the conversion can be summarized in two main elementary steps. The first one is the nucleophilic attack of the oxygen atom in water at the carbon center of the acetonitrile ligand to form the imino-coordinated complex **1b** with an energy barrier of 31.95 kcal/mol; then a proton transfer occurs from the hydroxy group to the imino nitrogen to form the acetamido-coordinated complex **1c**. The second step corresponds to an enol-to-keto tautomerization, which commonly exists in organic chemistry and is expected to have a very small energy barrier in solution.¹⁷

(16) Fung, W. K.; Huang, X.; Man, M. L.; Ng, S. M.; Hung, M. Y.; Lin, Z.; Lau, C. P. *J. Am. Chem. Soc.* **2003**, *125*, 11539.

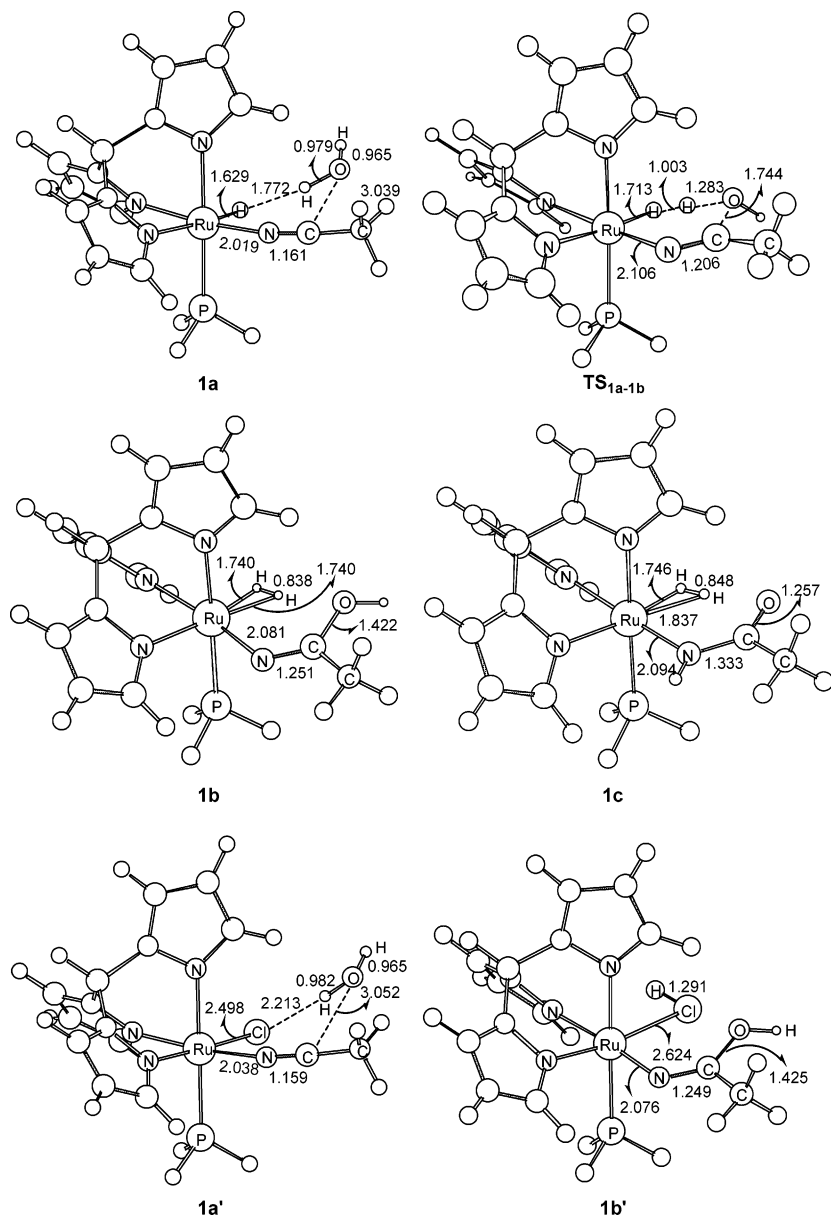


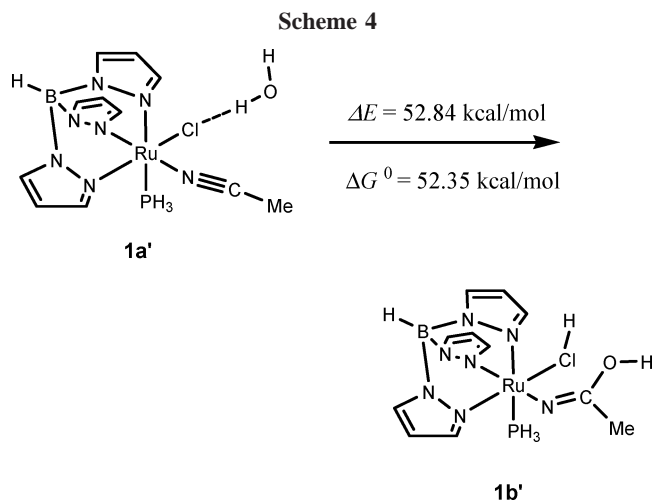
Figure 3. B3LYP-optimized structures for those species shown in Figure 2 and Scheme 3. Bond lengths are given in Å.

Figure 3 gives the optimized structures of species involved in the conversion process shown in Figure 2. The acetonitrile-coordinated complex **1a** is a hydride that contains dihydrogen bonding to a water molecule, with an H–H distance of 1.772 Å. The dihydrogen-bonding interaction is strengthened in the transition state TS_{1a-1b} , leading to shrinking of the H–H distance to 1.003 Å. Simultaneously, the distance between oxygen and the nitrile carbon decreases from 3.039 Å in **1a** to 1.744 Å in TS_{1a-1b} . These structural changes directly lead to the formation of the complex **1b**, in which a dihydrogen and an imino ligand are formed. The H–H distance in **1b** is 0.838 Å. The C≡N triple bond of nitrile in **1a** (1.161 Å) changes to a double bond in **1b** (1.251 Å). **1b** lies 16.10 kcal/mol higher in electronic energy than **1a**, but as expected, its keto form **1c** is 11.23 kcal/mol lower than **1a**. The most relevant changes

upon the enol-to-keto tautomerization concern the C–O bond, which decreases by 0.165 Å, and the C–N bond, which increases by 0.082 Å. From the conversion of **1a** to **1b**, we clearly see the structural change from a dihydrogen bond to a dihydrogen ligand, supporting the notion that the dihydrogen-bonding interaction assists the hydration process.

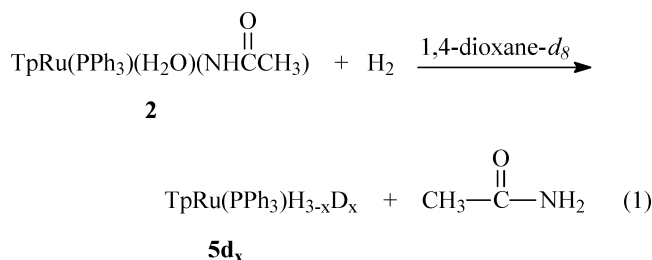
It is worth noting that, experimentally, such conversion of the acetonitrile ligand to the acetamido ligand is not observed for the chloro analogue of **1**. To gain insight into the reason, we calculated the reaction energy of $1a' \rightarrow 1b'$ shown in Scheme 4. Examination of the scheme shows that the imino-coordinated complex **1b'** is energetically located at 52.84 kcal/mol above the acetonitrile-coordinated complex **1a'**, indicating that **1b'** is thermodynamically very unstable in comparison with **1a'**. As a result, the chloro complex **1a'** does not undergo conversion of the acetonitrile ligand to the acetamido ligand. To understand why complex **1b'** is so unstable in comparison with complex **1a'**, we have checked the geometric and electronic properties of these complexes. It is noted that the formation of the H–Cl bond decreases the net negative charge of Cl dramatically from -0.56 to -0.12 , remarkably weakening the

(17) (a) Carey, F. A.; Sundberg, R. J. *Advanced Organic Chemistry Part A. Structure and Mechanisms*, 3rd ed.; Plenum Press: New York, 1990; pp 416–422. (b) Guthrie, J. P. In *The Chemistry of Enols*; Rappoport, Z., Ed.; Wiley: New York, 1990; pp 75–93. (c) Toullec, J. In *The Chemistry of Enols*; Rappoport, Z., Ed.; Wiley: New York, 1990; pp 323–398. (d) Keeffe, J. R.; Kresge, A. J. In *The Chemistry of Enols*; Rappoport, Z., Ed.; Wiley: New York, 1990; pp 399–480.



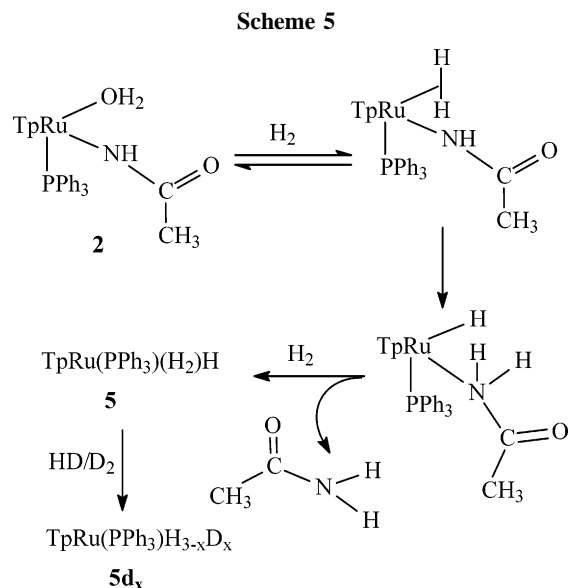
coordination capability of the ligand. Of course, this dramatic charge reduction results in the corresponding structural modifications (Figure 3), i.e., the increase of the Ru–Cl distance from 2.498 Å in **1a'** to 2.624 Å in **1b'**, which decreases the stability of the complex. In the case of complex **1b**, the dihydrogen ligand contributes to its stability in view of the fact that there are a large number of dihydrogen complexes reported in the literature.¹⁸

Reaction of 2 with H₂. The reaction of **2** in THF with H₂ (10 atm) was carried out in 1,4-dioxane-*d*₈ in a 5 mm pressure-valved NMR tube. After heating the tube at 110 °C overnight, ³¹P{¹H} and ¹H NMR spectroscopy showed that **2** was completely converted to TpRu(PPh₃)(H_{3-x})D_x (**5d_x**), the isotopomers of the dihydrogen hydride complex TpRu(PPh₃)(H₂)H (**5**) (eq 1); we have previously reported the synthesis and reactivity of **5** and **5d_x**.^{18f} The presence of free acetamide was evidenced by detection of a singlet at δ 1.97 ppm in the ¹H NMR spectrum. Apparently, H₂ underwent H/D exchange with 1,4-dioxane-*d*₈ to give HD and D₂, which were the sources of deuterium in the isotopomers (eq 1). We have, in fact, demonstrated that **5** catalyzes H/D exchange between H₂ and R–D (R–D = THF-*d*₈, C₆D₆, and diethyl ether-*d*₁₀).⁵



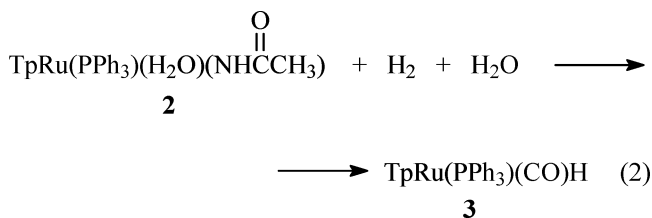
The formation of **5** from **2** and H₂ can be rationalized in terms of the reaction sequence shown in Scheme 5. Substitution of H₂O in **2** by H₂ forms the η²-dihydrogen intermediate (see **1c** in Figure 2), protonation of the acetamido ligand by η²-H₂ gives free acetamide, and subsequent coordination of another H₂ molecule yields the dihydrogen hydride complex. 1,2-Addition

(18) (a) Lin, Z.; Hall, M. B. *Coord. Chem. Rev.* **1994**, *135/136*, 845. (b) Kubas, G. J. *Metal Dihydrogen and σ-Bond Complexes*; Kluwer Academic/Plenum Publishers: New York, 2001. (c) Halcrow, M. A.; Chaudret, B.; Trofimenko, S. *J. Chem. Soc., Chem. Commun.* **1993**, 465. (d) Moreno, B.; Sabo-Etienne, S.; Chaudret, B.; Rodriguez, A.; Jalon, F.; Trofimenko, S. *J. Am. Chem. Soc.* **1995**, *117*, 7441. (e) Chan, W. C.; Lau, C. P.; Chen, Y. Z.; Fang, Y. Q.; Ng, S. M.; Jia, G. *Organometallics* **1997**, *16*, 34. (f) Chen, Y. Z.; Chan, W. C.; Lau, C. P.; Chu, H. S.; Lee, H. L.; Jia, G. *Organometallics* **1997**, *16*, 1241.



of coordinated H–H across the Ru–N bond of an amido-type ligand is well-documented.¹⁹

Reaction of 2 with H₂/D₂O. The reaction of **2** (in THF-*d*₈) with H₂ (10 atm) in the presence of excess D₂O was studied in a 5 mm pressure-valved NMR tube. It was found by ³¹P{¹H} NMR spectroscopy that after heating the tube at 110 °C for 6 h **2** was completely converted to a new species, which showed a slightly broadened singlet at δ 68.8 ppm. The chemical shift of this signal is identical to that of the signal corresponding to one of the two minor species (**3**) that we detected at the later stage of the **1**-catalyzed THF/D₂O exchange reaction (vide supra). We have, however, not been able to identify the organic products of the reaction by ¹H NMR spectroscopy. The solution was removed from the NMR tube, and the volatile materials were removed in vacuo. The residue was washed several times with hexanes and then subjected to ¹H and ³¹P{¹H} NMR studies, which revealed that **3** is in fact the carbonyl hydride complex TpRu(PPh₃)(CO)H that we previously reported.^{18f} The hydride ligand of **3** was partially deuterated, as indicated by the diminished integration of the upfield hydride signal. We are not sure, at this stage, of the reaction sequence that leads to the formation of **3** (eq 2). Complex **3** detected in the course of the **1**-catalyzed THF/D₂O exchange reaction probably resulted from the reaction of D₂O and the H₂ generated with **2**.



The catalytic activity of **2** in the H/D exchange reaction of THF with D₂O was studied; it was found that the complex was inactive for the exchange reaction. The **2**-catalyzed H/D reaction was again attempted in the presence of a small amount of H₂. ³¹P{¹H} NMR monitoring indicated that after an extended period

(19) (a) Sandoval, C. A.; Ohkuma, T.; Muñiz, K.; Noyori, R. *J. Am. Chem. Soc.* **2003**, *125*, 13490. (b) Conner, D.; Jayaprakash, K. N.; Cundari, T. R.; Gunnoe, T. B. *Organometallics* **2004**, *23*, 2724. (c) Abdur-Rashid, K.; Faatz, M.; Lough, A. J.; Morris, R. H. *J. Am. Chem. Soc.* **2001**, *123*, 7473. (d) Fryzuk, M. D.; Montgomery, C. D.; Rettig, S. J. *Organometallics* **1991**, *10*, 467.

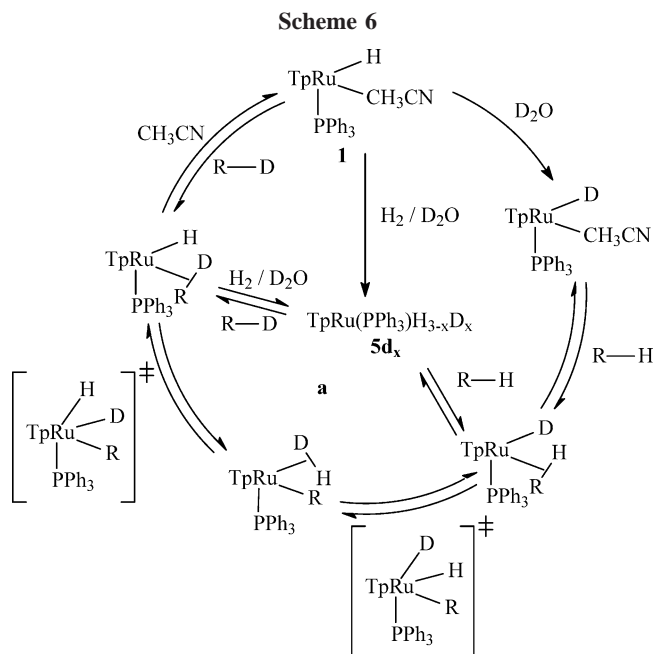


Table 4. H/D Exchange of Organic Solvents and D_2O by **1 under Hydrogen^a**

entry	substrate	% deuteration	total TON ^b	mol % of 1 ^c	
1	benzene	22	318	0.41	
2	toluene	aliphatic:	13	289	0.48
		<i>o</i> and <i>p</i> :	17		
		<i>m</i> :	26		
3	tetrahydrofuran	α hydrogen:	17	264	0.37
		β hydrogen:	7		
4	1,4-dioxane	20	408	0.40	
5	diethyl ether	α hydrogen:	13	400	0.48
		β hydrogen:	23		

^a Reaction conditions: catalyst, 0.0091 mmol; substrate, 0.2 mL; D_2O , 0.1 mL; pressure: $\text{H}_2 = 10$ atm; temperature, 110 °C; reaction time, 24 h. ^bTotal TON = mole of C–H bond activated/mole of catalyst. ^cRelative to the organic substrate.

of time minute amounts of **3** and the other unidentified species, **4**, were formed; the H/D exchange reaction, however, remained undetected. Thus, like **2**, **3** and **4** are also inactive for the H/D exchange reaction.

Mechanism of 1-Catalyzed H/D Exchange between R–H and D_2O under Ar. In light of our previous work on the **1**-catalyzed H/D exchange between CH_4 and R–D and the fact that the hydride ligand of **1** is rapidly deuterated by D_2O , we suggest that the H/D exchange between R–H and D_2O catalyzed by **1** proceeds via the sequence depicted in Scheme 6 (outer cycle). The hydride of **1** is acting as a go-between enabling the exchange of the deuterium of D_2O with the hydrogen of R–H. Ru–H is rapidly deuterated by D_2O to form Ru–D, which then undergoes H/D exchange with R–H; we have previously investigated the exchange process between Ru–D and R–H by density functional theory calculations (see also Scheme 1).⁵

In the course of the catalytic reaction, most of complex **1** is converted to **2d**, **3**, and **4**; these complexes are found to be inactive (vide supra). Probably, **1**, which is the active species, is present in such a small amount that it is not detectable by $^{31}\text{P}\{^1\text{H}\}$ and ^1H NMR spectroscopy.

Mechanism of 1-Catalyzed H/D Exchange between R–H and D_2O under H_2 . We have also studied the H/D exchange reactions of the substrates with D_2O under H_2 (10 atm) instead of Ar, the results of which are shown in Table 4. It can be seen that the overall results of the exchange reactions are similar to

those of the reactions under Ar. We monitored the behavior of the complex during a THF/ D_2O exchange reaction under H_2 with ^1H and $^{31}\text{P}\{^1\text{H}\}$ NMR spectroscopy. It was observed that **1** was readily converted to a mixture of the HD isotopomers $\text{TpRu}(\text{PPh}_3)(\text{H}_{3-x}\text{D}_x)$ (**5d_x**) of the dihydrogen hydride complex $\text{TpRu}(\text{PPh}_3)(\text{H}_2)\text{H}$ (**5**), and it remained the only NMR detectable metal-containing species throughout the reaction. Unlike the exchange reaction performed under Ar, the acetamido complex **2d** and the other two species **3** and **4** were not formed in the present case. Thus, in the exchange reaction under H_2 , **5d_x** is the active species of the catalytic system. The dihydrogen hydride complex **5** is fluxional,^{18f,20} the three hydrogen atoms interchange readily and are readily deuterated by D_2O . In fact, **5** is capable of catalyzing H/D exchange between H_2 and D_2O , and itself being deuterated to form **5d_x**. Transitional metal-catalyzed H/D exchange between H_2 and D_2O is well-documented.²¹

Similar to **1**, **5d_x** exchanges its Ru–D with R–H via the intermediacies of the σ -complexes (Scheme 6, cycle a). It is, however, suggested that **1** is more active than **5d_x** in the exchange reactions. The abundance of **5d_x** is much higher than that of **1** during the catalysis, and the former does not seem to degrade to other inactive species; however, due to its thermodynamic stability under H_2 , it is expected to be more difficult for **5d_x**, in comparison with **1**, to generate the R–H σ -complex via the exchange of a H_2 or HD ligand for the R–H molecule.

Conclusion

Continuing our work on C–H activation and H/D exchange between deuterated organic molecules and CH_4 with the solvento hydride complex $\text{TpRu}(\text{PPh}_3)(\text{CH}_3\text{CN})\text{H}$ (**1**), we have found that the catalytic systems based on **1** are capable of affecting the H/D exchange into organic compounds with D_2O . This work that we report here represents a new entry into the study of metal-catalyzed H/D exchange between organic molecules and D_2O ; reports on incorporation of deuterium into C–H bonds of organic molecules using D_2O as deuterium source are relatively rare. Our ruthenium systems are, at this stage, still far from being practically useful. However, our work indicates that transition metal solvento hydride complexes, by virtue of facile deuteration of the M–H bond with D_2O to form M–D and subsequent H/D exchange of the deuteride ligand with R–H, have high potentials to act as active catalysts for the deuteration of organic compounds using D_2O as deuterium source. Furthermore, the formation of the acetamido complex **2** might provide more insight into the mechanisms of the catalytic hydration reactions of nitriles with transition metal hydride complexes.

Experimental Section

Ruthenium trichloride, $\text{RuCl}_3 \cdot 3\text{H}_2\text{O}$, pyrazole, sodium borohydride, triphenylphosphine, and organic solvents were obtained from

(20) For fluxional dihydrogen hydride complexes, see, for example: (a) Bianchini, C.; Perez, P. J.; Peruzzini, M.; Zanobini, F.; Vacca, A. *Inorg. Chem.* **1991**, *30*, 279. (b) Bianchini, C.; Linn, K.; Masi, D.; Peruzzini, M.; Polo, A.; Al Vacca, Zanobini, F. *Inorg. Chem.* **1993**, *32*, 2366. (c) Heinekey, D. M.; Oldham, W. J., Jr. *J. Am. Chem. Soc.* **1994**, *116*, 3137. (d) Oldham, W. J., Jr.; Hinkle, A. S.; Heinekey, D. M. *J. Am. Chem. Soc.* **1997**, *119*, 11028.

(21) See, for example: (a) Chinn, M. S.; Heinekey, D. M. *J. Am. Chem. Soc.* **1990**, *112*, 5166. (b) Albeniz, A. C.; Heinekey, D. M.; Crabtree, R. H. *Inorg. Chem.* **1991**, *30*, 3632. (c) Kubas, G. J.; Burns, C. J.; Khalsa, G. R. K.; Van Der Sluys, L. S.; Kiss, G.; Hoff, C. D. *Organometallics* **1992**, *11*, 3390. (d) Kovács, G.; Nádasdi, L.; Laurenczy, G.; Joó, F. *Green Chem.* **2003**, *5*, 213. (e) Georgakaki, I. P.; Miller, M. L.; Darensbourg, M. Y. *Inorg. Chem.* **2003**, *42*, 2489. (f) Kovács, G.; Schubert, G.; Joó, F.; Pápai, I. *Organometallics* **2005**, *24*, 3059.

Aldrich. Triphenylphosphine was recrystallized from ethanol before use. Solvents were distilled under a dry nitrogen atmosphere with appropriate drying agents: hexane, diethyl ether, tetrahydrofuran, benzene, 1,4-dioxane, and toluene with sodium benzophenone; dichloromethane, acetonitrile, and chloroform with calcium hydride. The complexes $\text{TpRu}(\text{PPh}_3)(\text{CH}_3\text{CN})\text{H}^{18\text{e}}$ and $\text{TpRu}(\text{PPh}_3)(\text{CH}_3\text{-CN})\text{Cl}^{18\text{e}}$ were prepared according to literature methods. Deuterated NMR solvents, purchased from Armar, were dried with P_2O_5 . High-purity hydrogen and argon gases were supplied by Hong Kong Oxygen.

Proton NMR spectra were obtained from a Bruker DPX 400 spectrometer. Chemical shifts were reported relative to residual protons of the deuterated solvents. ^{31}P NMR spectra were recorded on a Bruker DPX 400 spectrometer at 161.70 MHz; chemical shifts were externally referenced to 85% H_3PO_4 in D_2O . $^{13}\text{C}\{^1\text{H}\}$ NMR spectra were taken on a Bruker DPX 400 spectrometer at 100.61 MHz; chemical shifts were internally referenced to C_6D_6 ($\delta = 128.1$ ppm). ^2H NMR spectra were taken on a Bruker DPX 400 spectrometer at 61.42 MHz; chemical shifts were internally referenced to TMS ($\delta = 0.00$ ppm). High-pressure NMR studies were carried out in commercial 5 mm Wilmad pressure-valved NMR tubes. Infrared spectra were obtained from a Bruker Vector 22 FT-IR spectrophotometer. Electrospray ionization mass spectrometry was carried out with a Finnigan MAT 95S mass spectrometer with the samples dissolved in dichloromethane. Elemental analyses were performed by M-H-W Laboratories, Phoenix, AZ.

H/D Exchange between Ru–H of **1 and D_2O .** A sample of $\text{TpRu}(\text{PPh}_3)(\text{CH}_3\text{CN})(\text{H})$ (**1**) (~5 mg) was loaded into a 5 mm NMR tube, which was then sealed with a septum. The tube was evacuated using a needle and filled with nitrogen for three cycles. THF (0.3 mL) and D_2O (8 μL) were added to the tube using syringes and needles. The solution was allowed to stand at room temperature for 10 min, after which the $^{31}\text{P}\{^1\text{H}\}$, ^1H , and ^2H NMR spectra of the solution were immediately recorded. The $^{31}\text{P}\{^1\text{H}\}$ NMR spectrum showed a slightly broadened singlet at δ 79.5 ppm, the chemical shift of which was identical to that of the signal of **1**. The ^1H NMR spectrum showed all the signals of **1** except the upfield hydride signal. The ^2H NMR spectrum showed a singlet at δ –13.94 ppm (br, Ru–D).

$\text{TpRu}(\text{PPh}_3)(\text{H}_2\text{O})(\text{NHC}(\text{O})\text{CH}_3)$ (2**).** A sample of $\text{TpRu}(\text{PPh}_3)(\text{CH}_3\text{CN})\text{H}$ (0.12 g, 0.20 mmol) was loaded into a two-necked round-bottom flask, which was then evacuated and flushed with nitrogen for four cycles. Freshly distilled THF (6 mL) and water (0.2 mL) were added to the flask, and the resulting solution was refluxed with stirring for 24 h. After cooling the solution to room temperature, the solvent was removed under vacuum and 10 mL of dichloromethane was added to the residue. The mixture was filtered to remove some insoluble solids; the filtrate was brought to dryness in vacuo to afford a green solid. The solid was washed with hexane (2 \times 6 mL) and 5:1 hexane/diethyl ether (2 \times 6 mL); it was collected and dried under vacuum for several hours at room temperature. Yield: 0.073 g (56%). Anal. Calcd (%) for $\text{C}_{20}\text{H}_{31}\text{-BN}_7\text{O}_2\text{PRu}$: C 53.39, H 4.79, N 15.03. Found: C 53.31, H 4.81, N 15.09. IR (KBr): $\nu(\text{C}=\text{O}) = 1540$ (m), $\nu(\text{N}-\text{H}) = 3337$ (m), $\nu(\text{B}-\text{H}) = 2461$ (m), ^1H NMR (400.13 MHz, C_6D_6 , 25 $^\circ\text{C}$): δ 2.05 (s, 3H; $\text{CH}_3\text{C}(\text{O})\text{NH}$), 4.67 (s, 1H; $\text{CH}_3\text{C}(\text{O})\text{NH}$), 5.93 (t, 1H of Tp), 5.97 (t, 1H of Tp), 6.28 (t, 1H of Tp), 6.87 (d, 1H of Tp), 7.29 (d, 1H of Tp), 7.78 (d, 1H of Tp), 7.85 (d, 2H of Tp), 8.24 (d, 1H of Tp) (all coupling constants for Tp proton resonances are about 2 Hz), 7.24, 7.68 (2 multiplets, 15H of PPh_3). $^{31}\text{P}\{^1\text{H}\}$ NMR (161.7 MHz, C_6D_6 , 25 $^\circ\text{C}$): δ 63.3 (s). $^{13}\text{C}\{^1\text{H}\}$ NMR (100.61 MHz, C_6D_6 , 25 $^\circ\text{C}$): δ 181.2 (s, $\text{CH}_3\text{C}(\text{O})\text{NH}$), 25.7 (s, $\text{CH}_3\text{C}(\text{O})\text{NH}$); other signals that are due to the Tp and PPh_3 ligands: δ 144.1, 143.8, 140.9, 135.5, 135.2, 134.8, 134.6, 133.6, 133.5, 128.1, 105.5, 105.4, 105.2, 105.0. ESI-MS (CH_2Cl_2): m/z 635 [$\text{M} - \text{H}_2\text{O}$] $^+$.

Catalytic H/D Exchange of Organic Compounds and D_2O

with $\text{TpRu}(\text{PPh}_3)(\text{CH}_3\text{CN})\text{H}$ under Ar or H_2 . A 5 mm pressure-valved NMR tube was loaded with $\text{TpRu}(\text{PPh}_3)(\text{CH}_3\text{CN})\text{H}$ (~6 mg) and then flushed with Ar for a few minutes. Freshly distilled organic solvent (0.2 mL) and degassed D_2O (0.1 mL) were added to the tube under Ar, and the tube was then pressurized with Ar or H_2 (10 atm). It was heated at 110 $^\circ\text{C}$ for 24 h. ^1H NMR spectroscopy was used to analyze the percentage of deuterium incorporation into the organic compound.

Use of ^1H NMR Spectroscopy to Determine Levels of Deuteration of the Organic Compound. For THF and 1,4-dioxane, which are miscible with water, no internal standard was used for the calculation of the level of deuteration. In the catalytic H/D exchange reaction, for example, between 1,4-dioxane and D_2O , the total number of hydrogen atoms (the exchanging hydrogen atoms of 1,4-dioxane and the residual hydrogen atoms of D_2O) is constant throughout the catalytic reaction. Based on the integrals of the residual D_2O peak and that of the exchanging hydrogen of 1,4-dioxane, before and after the exchange reaction, the percent deuterium incorporation into the organic compound can be calculated. For benzene, toluene, and diethyl ether, which are not miscible with D_2O , an internal standard, CH_2Cl_2 , was used for the determination of the levels of deuteration. In a typical experiment, a standard solution containing 10 μL of the organic compound and 10 μL of CH_2Cl_2 in CDCl_3 in an NMR tube was prepared. After the H/D exchange reaction of the organic compound with D_2O was stopped, the catalytic system was allowed to stand for several hours at room temperature to ensure good separation of the organic and aqueous phases. A CDCl_3 solution (the sample solution) containing 10 μL of the organic phase and 10 μL of the internal standard was prepared in an NMR tube. The ^1H NMR spectra of the sample solution and the standard solution were recorded. Based on the ratios of the integration of the signal of the exchanging hydrogen of the organic compound and that of the CH_2Cl_2 in the spectra of both solutions, the level of deuteration can be calculated.

Reaction of **2 with H_2 .** A sample of $\text{TpRu}(\text{PPh}_3)(\text{H}_2\text{O})(\text{NHC}(\text{O})\text{CH}_3)$ (**2**) (6 mg) loaded in a 5 mm pressure-valved NMR tube was dissolved in 1,4-dioxane- d_8 (0.3 mL); the tube was then pressurized with 10 bar of H_2 . The tube was heated at 110 $^\circ\text{C}$ for 16 h. ^1H and $^{31}\text{P}\{^1\text{H}\}$ NMR spectra were recorded, and it was evidenced from these spectra that **2** was completely converted to the known complex $\text{TpRu}(\text{PPh}_3)(\text{H}_{3-x})\text{D}_x$ (**5d_x**).

Reaction of **2 with $\text{H}_2/\text{D}_2\text{O}$.** A sample of $\text{TpRu}(\text{PPh}_3)(\text{H}_2\text{O})(\text{NHC}(\text{O})\text{CH}_3)$ (**2**) (6 mg) was loaded into a 5 mm pressure-valved NMR tube, to which THF (0.2 mL) and D_2O (0.05 mL) were added. The tube was then pressured with 10 bar of H_2 and heated at 110 $^\circ\text{C}$ for 6 h. The tube was cooled to room temperature, and the $^{31}\text{P}\{^1\text{H}\}$ NMR spectrum was recorded. $^{31}\text{P}\{^1\text{H}\}$ NMR (161.7 MHz, 25 $^\circ\text{C}$): δ 68.8 ppm (s). The solution in the NMR tube was then transferred to a 50 mL two-necked flask. The flask was flushed with nitrogen, and the solvent of the solution was removed in vacuo. The residue was washed with hexanes (2 mL \times 2). ^1H and $^{31}\text{P}\{^1\text{H}\}$ NMR spectra of a CDCl_3 solution of the residue were taken; these spectra confirmed that the residue is the known carbonyl hydride complex $\text{TpRu}(\text{PPh}_3)(\text{CO})\text{H}$ (**3**).

Crystallographic Structure Analysis of $\text{TpRu}(\text{PPh}_3)(\text{H}_2\text{O})(\text{NHC}(\text{O})\text{CH}_3)$ (2**).** Yellowish-green crystals of **2** suitable for X-ray diffraction study were obtained by layering of diethyl ether on a CH_2Cl_2 solution of the complex. A suitable crystal with dimensions 0.50 \times 0.40 \times 0.40 mm was mounted on a Bruker CCD area detector diffractometer and subject to Mo $\text{K}\alpha$ radiation ($\lambda = 0.71073$ Å) from a generator operating at 50 kV and 30 mA. The intensity data of **2** were collected in the range $2\theta = 3$ – 55° with oscillation frames of ψ and ω in the range 0– 180° . A total of 1321 frames were taken in four shells. An empirical absorption correction of the SADABS (Sheldrick, 1996) program based on Fourier coefficient fitting was applied. The crystal structure was solved by Patterson function methods and expanded by difference Fourier

syntheses, refined by full-matrix least-squares on F^2 using the Bruker Smart and Bruker SHELXTL program packages. All non-hydrogen atoms were refined anisotropically. Hydrogen atoms were placed in ideal positions and refined as riding atoms, except the two on the aqua ligand and the one on the boron atom of the Tp ligand, which were located by difference electron density map. The final cycle of the full-matrix least-squares refinement based on 7609 observed reflections ($I > 2\sigma(I)$) and 425 parameters converged to the R and R_w values of 0.0372 and 0.1042 for $\text{TpRu}(\text{PPh}_3)(\text{H}_2\text{O})(\text{NHC}(\text{O})\text{CH}_3)$.

Computational Details. All calculations were performed with Gaussian 03 packages.²² Molecular geometries of the model complexes, in which the phenyl groups of the phosphine ligand were modeled by hydrogen atoms, were optimized at the Becke3LYP level of density functional theory.²³ Each stationary point was adequately characterized by normal coordinate analysis (no imagi-

(22) Frisch, M. J.; Trucks, G. W.; Schlegel, H. B.; Scuseria, G. E.; Robb, M. A.; Cheeseman, J. R.; Zakrzewski, V. G.; Montgomery, J. A., Jr.; Stratmann, R. E.; Burant, J. C.; Dapprich, S.; Millam, J. M.; Daniels, A. D.; Kudin, K. N.; Strain, M. C.; Farkas, O.; Tomasi, J.; Barone, V.; Cossi, M.; Cammi, R.; Mennucci, B.; Pomelli, C.; Adamo, C.; Clifford, S.; Ochterski, J.; Petersson, G. A.; Ayala, P. Y.; Cui, Q.; Morokuma, K.; Malick, D. K.; Rabuck, A. D.; Raghavachari, K.; Foresman, J. B.; Cioslowski, J.; Ortiz, J. V.; Stefanov, B. B.; Liu, G.; Liashenko, A.; Piskorz, P.; Komaromi, I.; Gomperts, R.; Martin, R. L.; Fox, D. J.; Keith, T.; Al-Laham, M. A.; Peng, C. Y.; Nanayakkara, A.; Gonzalez, C.; Challacombe, M.; Gill, P. m. W.; Johnson, B.; Chen, W.; Wong, M. W.; Andres, J. L.; Gonzalez, C.; Head-Gordon, M.; Replogle, E. S.; Pople, J. A. *Gaussian 03*, Revision B.05; Gaussian, Inc.: Pittsburgh, PA, 2003.

(23) (a) Becke, A. D. *J. Chem. Phys.* **1993**, *98*, 5648. (b) Lee, C.; Yang, W.; Parr, R. G. *Phys. Rev. B* **1988**, *37*, 785.

nary frequencies for an equilibrium structure and one imaginary frequency for a transition structure). The intrinsic reaction coordinate (IRC) analysis was carried out to confirm that all stationary points are smoothly connected to each other. Gibbs free energy was obtained on the basis of the frequency calculations. The Ru, Cl, and P atoms were described using the LANL2DZ basis set including a double- ζ valence basis set with the Hay and Wadt effective core potential (ECP).²⁴ An additional f polarization shell was added for Ru, with an exponent of 1.235.²⁵ In the case of Cl and P, a d polarization shell was added, with exponents of 0.640 and 0.387, respectively.²⁶ The 6-31G basis set was used for other atoms, and polarization functions were added for atoms in the water molecule, the hydride ligand, and the CN group of the nitrile ligand.

Acknowledgment. We thank the Hong Kong Research Grant Council (Project Nos.: PolyU 5282/02P and PolyU 5008/05P) and the Hong Kong Polytechnic University for financial support.

Supporting Information Available: Tables of X-ray structural data, including data collection parameters, positional and thermal parameters, and bond distances and angles, for complex **2**. This material is available free of charge via the Internet at <http://pubs.acs.org>.

OM061045X

(24) Hay, P. J.; Wadt, W. R. *J. Chem. Phys.* **1985**, *82*, 299.

(25) Ehlers, A. W.; Böhme, M.; Dapprich, S.; Gobbi, A.; Höllwarth, A.; Jonas, V.; Köhler, K. F.; Stegmann, R.; Veldkamp, A.; Frenking, G. *Chem. Phys. Lett.* **1993**, *208*, 111.

(26) Höllwarth, A.; Böhme, M.; Dapprich, S.; Ehlers, A. W.; Gobbi, A.; Jonas, V.; Köhler, K. F.; Stegmann, R.; Veldkamp, A.; Frenking, G. *Chem. Phys. Lett.* **1993**, *208*, 237.